

# GABOR-PLASMA LENS FOCUSING FOR LEBT SYSTEMS\*

J. Pozimski, R. Dölling, A. Jakob, P. Groß and H. Klein

Institut für Angewandte Physik, Frankfurt

## Abstract

Low energy beam transport (LEBT) of high perveance ion beams suffers from high space charge forces. Spacecharge compensation reduces the necessary focusing force and the filling factor of the lenses and therefrom the emittance growth due to aberrations and inner fields. The use of electrostatic lenses is restricted due to decompensation by the electric fields. On the other side magnetic lenses suffer, for high mass ions, from necessary high magnetic fields and the resulting technical problems. A different approach for a LEBT system is a lens using a static non neutral plasma confined in a magnetic and electrostatic field configuration allowing strong electrostatic focusing together with partial conservation of spacecharge compensation. Modelling of the plasma in a way that lens aberrations are small is very difficult and the underlying theory is not fully understood. New measurements at low residual gas pressure as well as theoretical work and the results of numerical simulations will be discussed.

## 1 INTRODUCTION

Plasma lenses (using electrostatic or magnetic forces for focusing) have certain advantages compared with conventional lens systems. But so far they suffer from inhomogeneities in the plasma column which lead to beam aberrations and emittance growth. For the Gabor plasma lens (GPL) studies have been started in Frankfurt to investigate theoretically and experimentally the properties of electrostatic plasma focusing.

## 2 THEORY

Assuming a homogeneous density distribution in the lens the maximum electron charge density the 'classical limit' is given by the radial enclosure criteria [1]

$$\rho_{e, \max, rad} = \frac{e\epsilon_0 B_z^2}{2m_e} \quad (1)$$

neglecting all radial loss processes (i. g. by diffusion) and any longitudinal effects. An first estimation of the restrictions of electron charge density due to longitudinal losses ist given by

$$\rho_{e, \max, long} = \frac{4U_A \epsilon_0}{r_A^2} \quad (2)$$

with  $U_A$  the anodevoltage and  $r_A$  the anode radius, assuming homogeneous lens filling and the minimum potential on lens axis to be zero. Combining both criteria the maximum

\*Work supported by BMBF

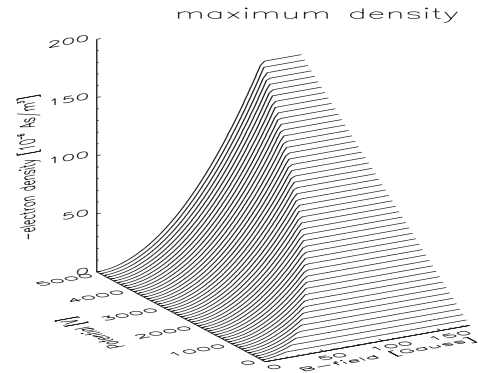


Fig. 1 : Theoretical maximum electron charge density in a Gabor plasma lens as a function of external parameters (Eq. (1)&(2)).

electron charge density as a function of the external parameters is shown in fig. 1. The electron density is a quadratic function of the magnetic field and linear with anode potential. Nevertheless hereby the electron density is overestimated by a factor of 3-5 compared with measurements. This behaviour is well known in literature for similar confined plasmas [2]. Therefore a computer code has been developed to simulate the local electron density in the GPL in a self consistent manner. Longitudinal losses are estimated from the density of Boltzmann distributed electrons at the wall and their thermal velocity. It is further (somewhat arbitrarily) assumed that the mean lifetime of electrons given by this losses equals the thermalization time of the electrons due to collisions. Radial losses caused by diffusion of electrons across magnetic field lines are neglected.

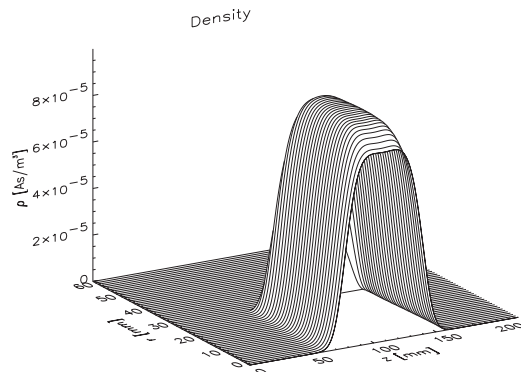


Fig. 2 : Numerically simulated selfconsistent electron density distribution in a Gabor plasma lens ( $B_z=90 \cdot 10^{-4}$  T,  $U_A=5$  kV,  $I_{loss}=1 \mu A$ ).

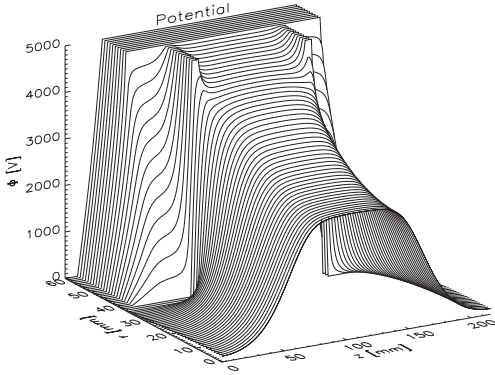


Fig. 3 : Potential distribution corresponding to fig. 2.

### 3 NUMERICAL SIMULATIONS

Fig. 2 shows the simulated electron density distribution inside the GPL assuming equilibrium state for an anode voltage of 5 kV and the magnetic field of  $90 \cdot 10^{-4}$  T. The longitudinal electron losses result to 1  $\mu$ A. The electron density on lens center is comparable to the results of the classic theory (Eq. 1). The electrons are longitudinally (due to the temperature and losses) and radially (reaching the classical limit) concentrated on the lens center. Fig. 3 shows the potential distribution inside the lens including the space charge of the electrons. To investigate the behaviour of the electron distribution inside the lens and of electron losses for varied anode voltage and magnetic field strength multiple simulations have been performed. Fig. 4 shows the dependency of the longitudinal electron losses on the electron density on lens axis in equilibrium state. Only for loss rates below 100  $\mu$ A the electrons can thermalize. For higher electron loss rates (and therefore production rates) the electron density on axis weakly increases. This is due to the fact that the electron loss function is dominated by electron temperature not by electron density. Fig. 5 shows the influence of the anode voltage on the electron density for constant magnetic field. The electron density is in first order

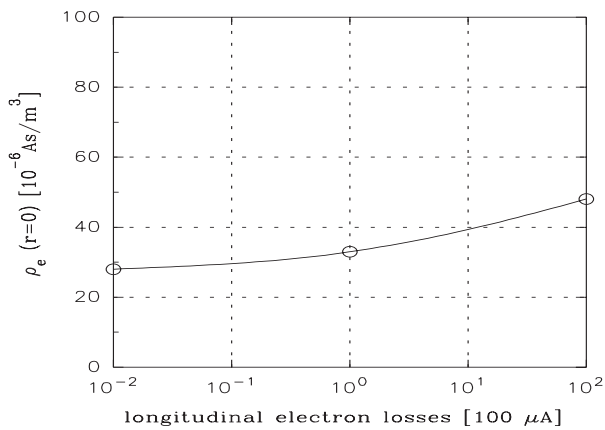


Fig. 4: Numerical simulated development of electron density in equilibrium state in a GPL as a function of longitudinal electron losses ( $B_z=500 \cdot 10^{-4}$  T,  $U_A=5$  kV).

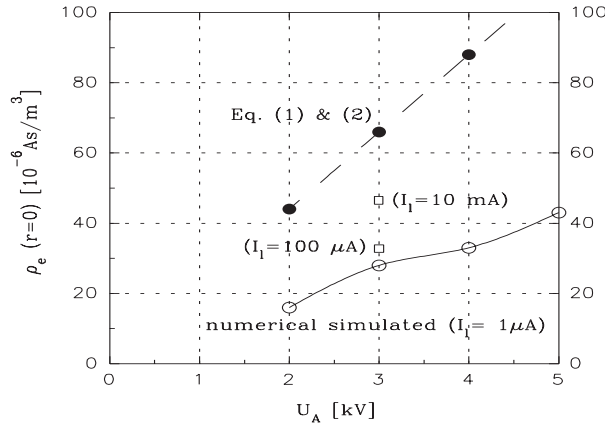


Fig. 5: Numerical simulated development of electron density in equilibrium state in a GPL as a function of anode voltage ( $B_z=500 \cdot 10^{-4}$  T,  $I_{\text{loss}}=1 \mu$ A)..

approximation linear with the anode voltage (like in the semi classical theory (Eq. (1) & (2))). In contrary the measurements show a slightly underlinear behavior. This can be explained by increasing radial losses due to higher electric fields (diffusion is proportional to  $E/B$ ). Fig. 6 shows the electron density for fixed anode voltage as a function of the magnetic field. Below a minimum field strength all electrons are radially expelled solely by the action of the external electric field (classical limit). Above the critical field strength the electron density on axis at first drastically rises and then becomes constant. For increasing magnetic field the diameter of the electron cloud and therefore the focusing capabilities are increasing too.

### 4 MEASUREMENTS

Beam measurements using a LEBT with two solenoids for beam formation have been performed [3,4] at low residual gas pressure (minimizing the effects of electron production and the influence of the space charge of the residual gas ions). The beam was matched parallel with a diameter of appr. 45 mm into the lens. Fig. 7 shows the result of an emittance measurement with the beam focussed to minimum radius at measurement point by the GPL. The

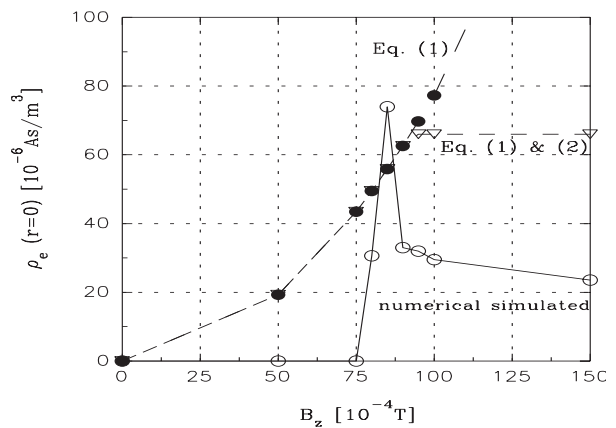


Fig. 6: Numerical simulated development of electron density in equilibrium state in a GPL as a function of magnetic field strength ( $U_A=3$  kV,  $I_{\text{loss}}=1 \mu$ A).

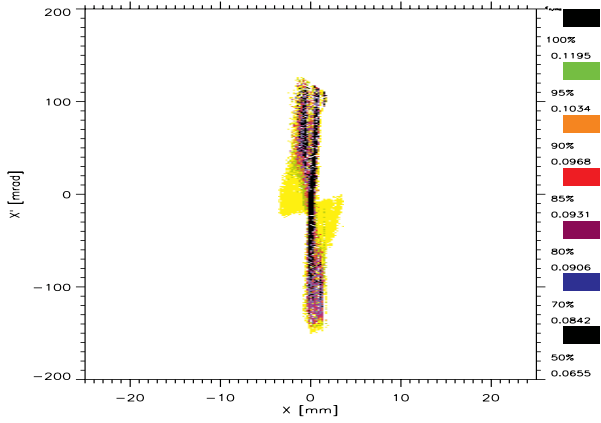


Fig. 7 : Emittance pattern of a  $\text{He}^+$  beam (10 keV, 3.6 mA) measured appr. 60 mm behind the GPL (5 kV,  $90 \cdot 10^{-4}$  T).

performance of the lens is capable to fulfill the injection requirements of an RFQ. Comparison with a numerical transport simulation (see fig. 8) show that the aberration at low angles are caused by inhomogeneous electron density.  $\kappa$  the quotient of the indirectly measured electron densities and the classical theory as a function of the magnetic field strength (Fig. 9) show similar behaviour compared with the results of the numerical simulations (Fig. 6). Measurements of the degree of compensation show a decrease (from 80 % compensation to 20 %) compared with transport using only magnetic fields. For different external fields the loss channel dominating the behavior of the lens changes and therefrom the compensation degree. The emittance growth varies from 20-300 % dominated by time varying space charge forces due to ion source noise and by radial plasma inhomogeneity. The second is mainly influenced by lens geometry and therefore can be optimized through simulation. In a second experiment the LEBT has been modified by inserting to anodes into the solenoids using the two solenoids for delivering the magnetic fields for the GPL. Using Argon as beam ions the modified solenoids show a higher focusing strength with the GPL effect than without. Fig. 10 shows an emittance measurement with an already overfocussed beam (at 2 kV,  $120 \cdot 10^{-4}$  T) where the

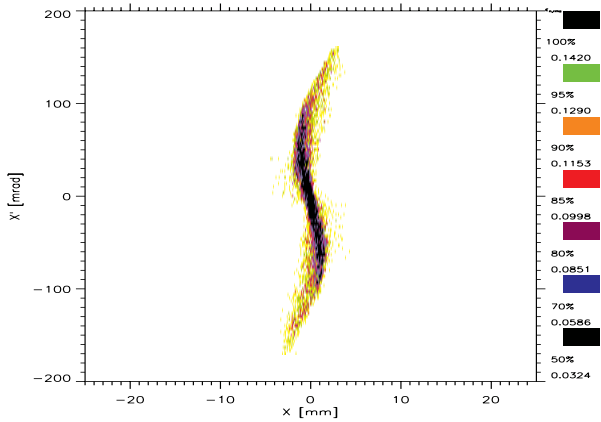


Fig. 8 : Calculated emittance pattern of a  $\text{He}^+$  beam (10 keV, 3.6 mA) appr. 60 mm behind the GPL (5 kV,  $90 \cdot 10^{-4}$  T) using 10000 particles for transport calculation.

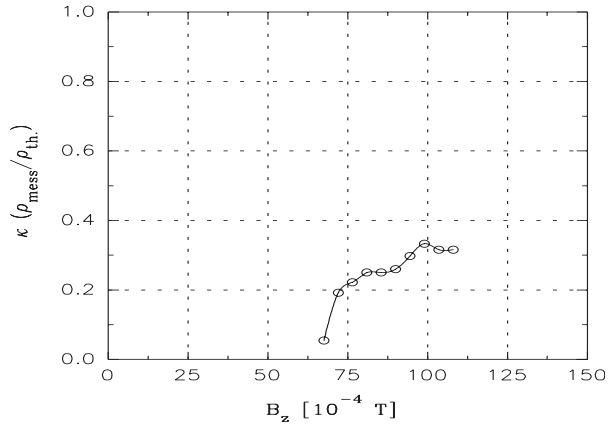


Fig. 9 : Development of filling factor  $\kappa$  as a function of the magnetic field strength (gained by comparison of measured data with classical theory (eq. 1)).

solenoids can deliver a parallel beam at maximum field strength only (at 0.6 & 0.8 T).

## 5 CONCLUSIONS

Measurements have proofed that GPLs are able to focus a positive ion beam of high perveance and medium mass at 10 keV beam energy fulfilling the requirements for injection into a RFQ. The emittance growth is (at optimum external parameters) comparable with magnetic solenoids and for high currents better than conventional electrostatic einzel lenses. Numerical simulations show an improved quality of transport capability forecast especially for plasma states where radial diffusion processes are neglectible. Experiments are planned with higher masses ( $\text{Bi}^+$ ) at higher energy to investigate the possibilities for an inertial fusion driver LEBT. In a next step the radial diffusion processes will be included into the simulations.

## 6 REFERENCES

- [1] D. Gabor, Nature 160 (1947) 89
- [2] D. P. Xi, Physika Scripta 39, 105 (1989)
- [3] J. Pozimski et. Al. Proc. LINAC Conf. 1996, Geneva
- [4] J. Pozimski , Dissertation in preparation (IAP, 1997)

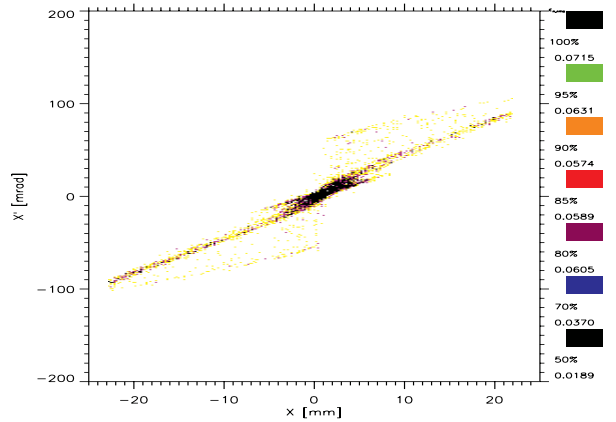


Fig. 10 : Emittance pattern of a  $\text{Ar}^+$  beam (10 keV, 400  $\mu\text{A}$ ) measured appr. 330 mm behind the second solenoid (used as GPL at 2 kV ,  $120 \cdot 10^{-4}$  T).